Reconsideration of surface tension and phase state effects on CCN activity based on the AFM measurement

Chun Xiong[1], Xueyan Chen[3], Xiaolei Ding[4], Binyu Kuang[1], Xiangyu Pei[1], Zhengning Xu[1], Shikuan Yang[3], Huan Hu[4*], Zhibin Wang[1,2,5*]

[1]College of Environmental and Resource Sciences, Zhejiang University, Zhejiang Provincial Key Laboratory of Organic Pollution Process and Control, Hangzhou, China

[2]ZJU-Hangzhou Global Scientific and Technological Innovation Center, Hangzhou, China

[3]Institute for Composites Science Innovation, School of Materials Science and Engineering, Zhejiang University, Hangzhou, Zhejiang 310027, China

[4]Zhejiang University-University of Illinois at Urbana-Champaign Institute, International Campus, Zhejiang University, Haining 314400, China

[5]Key Laboratory of Environment Remediation and Ecological Health, Ministry of Education, Zhejiang University, Hangzhou, China

Correspondence to: Zhibin Wang (wangzhibin@zju.edu.cn) and Huan Hu (huanhu@intl.zju.edu.cn)

Abstract. Dicarboxylic acids are ubiquitous in atmospheric aerosol particles, but their roles as surfactants in cloud condensation nuclei (CCN) activity remain unclear. In this study, we investigated CCN activity of inorganic salt (sodium chloride and ammonium sulfate) and dicarboxylic acid (including malonic acid (MA), phenylmalonic acid (PhMA), succinic acid (SA), phenylsuccinic acid (PhSA), adipic acid (AA), pimelic acid (PA) and octanedioic acid (OA)) mixed particles with varied organic volume fraction (OVF), and then directly determined their surface tension and phase state at high relative humidity (over 99.5%) by atomic force microscopy (AFM). Our results show that CCN derived κ_{CCN} of studied dicarboxylic acids ranged in 0.003-0.240. A linearly positive correlation between κ_{CCN} and solubility was obtained for slightly dissolved species, while negative correlation was found between κ_{CCN} and molecular volume for highly soluble species. For most inorganic salt/dicarboxylic acid (MA, PhMA, SA, PhSA and PA), a good closure within 30% relative bias between κ_{CCN} and chemistry derived κ_{Chem} was obtained. However, κ_{CCN} values of inorganic salt/AA and inorganic salt/OA systems were surprisingly 0.3-3.0 times higher than κ_{Chem}, which was attributed to surface tension reduction as AFM results showed that their surface tensions were 20%-42% lower than that of water (72 mN m^{-1}). Meanwhile, semisolid phase states were obtained for inorganic salt/AA and inorganic salt/OA and also affected hygroscopicity closure results. Our study highlights that surface tension reduction should be considered to investigate aerosol-cloud interactions.

1 Introduction

Atmospheric particles can indirectly affect global climate through their impacts on aerosol-cloud interaction by serving as cloud condensation nuclei (CCN) (Rosenfeld et al., 2014). Exploring the factors affecting CCN activation can help to

understand the aerosol-cloud interactions and thus decrease the uncertainty in the assessment of climate model. Köhler theory provides the basis for linking CCN activity with aerosol thermodynamic properties (Köhler, 1936), in which size and chemical composition are key factors to determine the activation of aerosol particles. Previous studies pointed out that aerosol number size distribution was essential to determine CCN concentration other than composition (Dusek et al., 2006; Gunthe et al., 2009; Rose et al., 2010). The role of particle chemistry in the activation process, however, is still debatable due to the complexity of chemical constitution (Bhattu and Tripathi, 2015; Noziere, 2016).

Single parameter κ was introduced in Köhler theory to describe hygroscopicity of aerosol particles (Petters and Kreidenweis, 2007). κ-Köhler theory usually performed well in predictions of hygroscopicity and CCN number concentration (Rose et al., 2010; Kawana et al., 2016; Cai et al., 2020; Zhang et al., 2020). However, remarkable offset was also found because of the simplifications in κ-Köhler theory (Ruehl et al., 2016; Ovadnevaite et al., 2017). For example, aerosol droplet is assumed to be diluted near activation and surface tension is usually simply treated as that of pure water, which is sometimes not reasonable in the presence of atmospheric surfactants (Lowe et al., 2019). Many previous studies investigated surface tension effect of atmospheric surfactant on aerosol CCN activity (Ruehl and Wilson, 2014; Ruehl et al., 2016; Ovadnevaite et al., 2017). At Mace Head, Ovadnevaite et al. (2017) observed significant underestimation of CCN number concentration (one tenth) in a nascent ultrafine mode event with high organic mass fraction (55%). The underestimation was improved by applying lower water surface tension (~ 68% of water surface tension). For surfactant sodium octyl sulfate, Peng et al. (2022) found that CCN-derived κ_{CCN} was around 2.4 times larger than the growth factor derived κ_{GF}, which was ascribed to surface tension reduction and solubility limit. Though established thermodynamic models considering surface tension reductions such as compressed film model (Ruehl et al., 2016) and liquid-liquid phase separation model (Ovadnevaite et al., 2017; Liu et al., 2018) explained the discrepancies of CCN activity or CCN number concentration closure, dataset of direct measurement of surface tension for submicron particles are very rare.

Dicarboxylic acids are ubiquitous in atmospheric aerosol particle as a main contributor to organic aerosol mass (mass contribution to total particulate carbon exceeds 10% in remote area) (Römpp et al., 2006; Ho et al., 2010; Hyder et al., 2012). Primary emission (e.g. biomass burning and fossil fuel combustion) and secondary formation (e.g. photooxidation of unsaturated fatty acids) were major sources of dicarboxylic acids (Ho et al., 2010). Furthermore, dicarboxylic acids are also known as important atmospheric surfactants and their surface activities in water solutions showed a positive relation with carbon number (Aumann et al., 2010). Currently, most studies investigated surface tension effect of dicarboxylic acids on CCN activation by measuring surface tension of their solutions and using models based on solution results (Lee and Hildemann, 2013, 2014; Ruehl et al., 2016; Zhang et al., 2021; Vepsäläinen et al., 2022). However, the values derived from bulk solutions may not be a reasonable representation for aerosol particles because their high surface-to-volume ratio may affect the distribution of surfactant between surface and bulk (Ruehl et al., 2010; Ruehl and Wilson, 2014). Recently, new methods of surface tension measurement for particles were introduced such as microfluid (Metcalf et al., 2016) and optical tweezers (Bzdek et al., 2020), but their samples were micrometre size droplets. Morris et al. (2015) presented a way to directly measure

surface tension of submicron particles under controlled relative humidity (RH) by atomic force microscopy (AFM). Later, AFM was further reported to be an important tool to probe phase state of individual particles (Lee et al., 2017a; Lee et al., 2017b; Lee and Tivanski, 2021). However, most measurements using AFM were performed with RH under 95% (Morris et al., 2015; Lee et al., 2017b; Ray et al., 2019; Lee et al., 2020) but rarely in higher RH conditions. When RH approaches 100%, Kelvin effect becomes comparable to the Raoult effect in controlling hygroscopicity, so measurements around 100% RH can help resolve discrepancies between sub-saturated hygroscopicity and CCN activity (Ruehl and Wilson, 2014).

In this study, we firstly measured CCN activities of internal mixtures containing inorganic salt and dicarboxylic acid. Then, we directly obtained their surface tension and phase states by AFM under relatively high RH (over 99.5%). Our results could provide directly dataset of surface tension and phase state of inorganic salts-dicarboxylic acids internal mixed particles, which would help to decrease the uncertainty for climate models.

2 Methods

2.1 Experiments

2.1.1 Chemicals

Nine used compounds in the present study were sodium chloride (NaCl), ammonium sulfate (AS), malonic acid (MA), phenylmalonic acid (PhMA), succinic acid (SA), phenylsuccinic acid (PhSA), adipic acid (AA), pimelic acid (PA) and octanedioic acid (OA). Their relevant properties investigated in this study were summarized in **Table 1**.

2.1.2 CCN activity measurements

The measurement setup is shown in **Fig. 1**. In brief, particles containing single and mixed chemicals were generated by clean and particle-free compressed air with water solutions (~ 1‰) by a constant output atomizer (TSI 3079A). The solutions were prepared by using ultrapure water (Millipore, resistivity $\leq 18.2 M\Omega$). After drying (RH < 15%), monodispersed aerosol particles were obtained by differential mobility analyzer (DMA, TSI 3081) with the sheath to sample flow ratio of 10, and then were split between a condensation particle counter (CPC, TSI 3772) for measuring number concentration of total particles (N_{CN}) and a Cloud Condensation Nuclei Counter (CCNC, DMT-200) for measuring number concentration of CCN (N_{CCN}).

In this study, the CCNC was operated in Scanning Flow CCN Analysis (SFCA) mode, which was introduced elsewhere (Moore and Nenes, 2009). In short, the pressure and ΔT of CCNC were kept constant, the flow rate was continuously and linearly varied from 0.2 L min^{-1} to 1 L min^{-1} or vice versa (1-0.2 L min^{-1}) within 125 s and the interval time for stabilization is 25 s. The supersaturations in CCNC was calibrated under four ΔT (4K, 6K, 10K and 18K). We obtained sigmoidal curves of activation ratio (N_{CCN}/N_{CN}) versus flow rate, then fitted the inflection point of the curves as critical flow rate Q_{50}. Ammonium sulfate was used to determine supersaturation ratio with an activity parameterization Köhler model AP3 as suggested by Rose et al. (2008). The calibration results were showed in **Fig. S1**.

2.1.3 Surface tension measurements

As shown in **Fig.1**, samples for AFM analysis were collected through deposition by impaction with an eight stage non-viable particle sizing sampler (Models BGI20800 Series, BGI Incorporation) onto hydrophobically silicon wafers. The hydrophobically silicon wafers are with polydimethylsiloxane brush surface, so solute can be collected into the solute aggregate on the surface after water evaporation when RH varies (especially RH decreases) (Ding et al., 2020). The aerodynamic size of collected particles was ranged in 0.4 μm-1 μm (50% efficiency). The substrate deposited particles were stored under dry condition (RH < 10%) and most of the samples were studied at the same day to avoid possible sample aging. Surface tension measurement was performed using an AFM system (Cypher ES, Asylum Research). Cypher ES contains a small cell with air inlet and outlet, it enables to scan samples under different environmental conditions such as RH. RH in cell was achieved and maintained by humidified flow. RH in cell was measured by a RH sensor (SHT 85, ± 1.5% uncertainty, Sensirion Inc.). Custom-built high aspect ratio (HAR) platinum AFM probes with constant diameter and nominal spring constant of ~ 3.0 N m^{-1} were used for particle imaging and surface tension measurements (**Fig. S2**) (Morris et al., 2015). The platinum nanoneedles could well measure surface tension of pure water and 1, 3-propanediol (**Fig. S3**). The procedures of making nanotips were detailly described in Ding et al. (2022) and a brief description was given here. Firstly, dual-beam-focused ion beam (FIB, ZEISS crossbeam 350) microscope was used to etch the top of the tip (Multi75Al-G purchased from BudgetSensors Inc.), making the etched tip flat. Then, FIB was used to deposit a cylindrical metal platinum column (100 nm-500 nm diameter) on the flat surface of the etched tip.

The principles of surface tension measurement using AFM were described elsewhere (Yazdanpanah et al., 2008; Morris et al., 2015; Lee et al., 2017a). Collected samples were firstly imaged in tapping mode to locate individual particles under dry condition (RH < 10%), then the RH gradually increased to over 99.5% in ~ 40 minutes (**Fig.S4**). Force-distance plots of droplet were obtained by contact mode. A tip velocity of 1-2 μm s^{-1} and dwell time of 1-2 seconds were used for all measurements (Kaluarachchi et al., 2021). More than 10 force plots were collected on at least 5 individual droplets in order to decreased the uncertainties (e.g. sensor accuracy). Precise diameter of nanoneedle was calibrated by measuring surface tension of pure water by adding a water droplet (2-3 mm height) onto silicon wafer (Kaluarachchi et al., 2021). New probe was used for different chemicals in order to avoid possible contamination of the AFM probe. However, it should be noted that the potential uncertainty introduced due to the different particle diameter in CCN activity (ranged in 50~260 nm) and AFM experiments (0.4-1μm) is not taken into account, because the size dependence of surface tension is not significant unless the solution droplets are smaller down to 6 nm (Cheng et al., 2015).

2.2 Theory

Based on κ-Köhler theory, hygroscopicity parameter κ_{CCN} for individual pure component and mixed aerosol can be calculated by:

126 $$\kappa_{\mathrm{CCN}} = \frac{4A^3}{27D_d^3 ln^2(1+s_c)}, A = \frac{4M_w \sigma_w}{RT\rho_w} \tag{1}$$

127 where σ_w, M_w and ρ_w are surface tension, molecular weight and density of water, respectively. R is universal gas constant and

128 T is temperature (298.15K). s_c is critical supersaturation ratio. D_d is dry diameter. In addition, hygroscopicity κ of

129 multicomponent chemical system can also be calculated assuming a Zdanovskii, Stokes, and Robinson (ZSR) simple mixing

130 rule. κ based on the chemical composition (κ_{Chem}) of mixed aerosol was calculated by:

131 $$\kappa_{\mathrm{Chem}} = OVF \cdot \kappa_{\mathrm{org,CCN}} + (1 - OVF) \cdot \kappa_{\mathrm{inorg,CCN}} \tag{2}$$

132 where $\kappa_{\mathrm{org,CCN}}$ and $\kappa_{\mathrm{inorg,CCN}}$ are obtained κ_{CCN} values of single organic acid and inorganic salt. OVF indicates the organic

133 volume fraction of mixed particles

134 As described by Morris et al. (2015), the basis of surface tension measurement for a liquid droplet by AFM was calculated by:

135 $$\sigma = \frac{F_r}{2\pi r} \tag{3}$$

136 where F_r is the retention force to break the meniscus by the tip of AFM probe, r is the radius of the AFM probe tip, and σ is

137 surface tension of the droplet. The retention force is the force difference before and after the probe was just retracted from the

138 droplet.

139 **3 Results and discussion**

140 **3.1 κ_{CCN} of single component**

141 κ_{CCN} values for single component aerosols were summarized in **Table 2**. κ_{CCN} of NaCl, AS, MA, SA and AA were 1.325 ±

142 0.038, 0.562 ± 0.059, 0.240 ± 0.036, 0.204 ± 0.023 and 0.008 ± 0.001, respectively, being overall consistent with previous

143 results (Petters and Kreidenweis, 2007; Kuwata et al., 2013). κ_{CCN} of NaCl and MA were slightly higher while AS was slightly

144 lower than those reported in Petters and Kreidenweis (2007). This may be ascribed to the solute purity (Hings et al., 2008).

145 Based on the same reason, κ_{CCN} of PA (0.112 ± 0.010) and OA (0.003 ± 0.0002) were 20% lower and twice higher than those

146 reported by Kuwata et al. (2013), respectively. κ_{CCN} values of PhMA and PhSA were 0.183 ± 0.032 and 0.145 ± 0.017,

147 respectively, which was firstly reported to our knowledge.

148 Solubility and molar volume of dicarboxylic acids were essential factors influencing their hygroscopicity (Kumar et al., 2003;

149 Han et al., 2022). Therefore, solubility criteria of 100 g/L was used in our study to distinguish the effect of solubility of highly

150 soluble (with water solubility over 100 g L^{-1}) and slightly soluble organics (with water solubility below 100 g L^{-1}) on their

151 hygroscopicity, according to Kuwata et al. (2013) and Luo et al. (2020). As showed in **Fig. 2a**, the κ_{CCN} values for highly

152 soluble components decreased linearly with increased molecular volumes. This trend was similar to κ_{CCN} values for sugar as

153 well as dicarboxylic acids reported by Chan et al. (2008). In **Fig. 2b**, κ_{CCN} values of sparely soluble components (AA, PA, SA

154 and OA) showed an increased trend with solubility, as organic matter with the higher water solubility would dissolve more

155 and have a higher molar concentration, resulting in reduction in water activity and higher hygroscopicity (Luo et al., 2020;

156 Han et al., 2022).

157 Organic functional group could also affect hygroscopicity (Suda et al., 2014; Petters et al., 2017). κ_{CCN} of PA (0.112) was

158 higher than those of AA (0.008) and OA (0.003), which is contrary to results in Suda et al. (2014) and Petters et al. (2017) that

159 hygroscopicity decreased with increased number of methylene. This phenomenon was attributed to the odd-even effect of

160 dicarboxylic acids, that is, diacids with odd numbers of carbon atoms being more soluble than those with adjacent even

161 numbers (Zhang et al., 2013). Furthermore, κ_{CCN} values of PhMA and PhSA were both lower than that of MA and SA,

162 respectively, indicating that the addition of phenyl showed negative effects on hygroscopicity. The addition of phenyl

163 substitution increased the molar volumes of MA and SA and may contribute to the drops of hygroscopicity (Petters et al.,

164 2009).

3.2 κ_{CCN} of inorganic salt-dicarboxylic acid mixed components

166 **Figure 3** presents the κ_{CCN} values of inorganic salt/dicarboxylic acid mixed particles with varied organic volume fractions

167 (OVF). Overall, κ_{CCN} of each inorganic salt/dicarboxylic acid system showed a decreased trend with increased OVF. For

168 example, κ_{CCN} of AS/MA particles with OVF of 57%, 73% and 88% were 0.399, 0.373 and 0.336, respectively. Larger fractions

169 of dicarboxylic acids (with low hygroscopicity compares to inorganic salts) caused more decrease in hygroscopicity of

170 inorganic/dicarboxylic acid system. As for inorganic salt/dicarboxylic acid systems with same OVF, κ_{CCN} values of systems

171 of AS/MA, AS/SA, AS/PhMA, AS/PhSA and AS/PA with 57% OVF were 0.399, 0.382, 0.364, 0.340 and 0.334, following

172 the order of κ_{CCN} values of single dicarboxylic acid (**Fig. 3a**). However, κ_{CCN} values of NaCl/AA and NaCl/OA mixed particles

173 with OVF of 60% were 0.734 and 0.685, even higher than that of NaCl/MA (0.639), demonstrating an opposite trend with

174 respect to those of single components. This discrepancy could be ascribed to surface tension reduction because AA and OA

175 showed different physical properties (e.g. deliquescence point, surface activity and solubility) when comparing with the other

176 organics, thus may result in distinct microphysics processes during interactions with inorganic salts and water content. AA and

177 OA own lowest solubilities and high deliquescence RH (**Table1**) among experimental dicarboxylic acids, which potentially

178 lead to their weak CCN activities (Hings et al., 2008). However, inorganic salts were found to facilitate the deliquescence of

179 dicarboxylic acid (Bilde and Svenningsson, 2004; Sjogren et al., 2007; Minambres et al., 2013). AS/AA mixed particles

180 deliquescence under 78%-83% RH with mass fractions of AA between 50%-80% (Sjogren et al., 2007). Small amount of NaCl

181 (2% mass faction) could notably decrease s_c of AA with 80 nm dry diameter from over 2% to ~0.6% (Bilde and Svenningsson,

182 2004). Thus, addition of inorganic salts facilitates deliquescence of OA and AA under lower RH, further promotes their phase

183 state transition from solid to liquid (or semisolid), and their surface tension would be reduced. Based on surface tension results

184 of water solutions, Aumann et al. (2010) reported that surface activities of dicarboxylic acids were increased with their carbon

185 number. Therefore, surface tensions of inorganic salts/AA and inorganic salts/OA may decrease more than the rest acids

186 containing particles, resulting in their relatively higher κ_{CCN}. This indication was further confirmed by AFM surface tension
187 measurement, as discussed in Section 3.4.

3.3 Closure study between κ_{CCN} and κ_{Chem}

189 κ_{CCN} and κ_{Chem} values for inorganic salt/dicarboxylic acid mixed particles were showed in **Fig. 4**. κ_{CCN} values of inorganic salt
190 and most dicarboxylic acids (MA, PhMA, SA, PhSA and PA) mixed particles could be predicted by ZSR mixing rule with
191 relative difference below 30% (**Fig. 4a**). Similar results have been found in previous lab and filed studies (Ruehl et al., 2012;
192 Kuwata et al., 2013; Wu et al., 2013; Dawson et al., 2016; Nguyen et al., 2017; Ovadnevaite et al., 2017), indicating that semi-
193 experimental ZSR mixing rule could be a useful method to predicted mixed particles hygroscopicity and CCN activation. For
194 instance, Dawson et al. (2016) reported consistence between κ_{CCN} and κ_{Chem} for NaCl/xanthan gum and $CaCO_3$/xanthan gum
195 mixed particles within 10% uncertainty. Wu et al. (2013) also obtained same closure results in a field study at central Germany,
196 for particles containing 60%-80% organic mass fraction and 30%-50% inorganic salts. Meanwhile, CCN studies also found
197 that using κ_{Chem} could well predict measured CCN number concentration (Juranyi et al., 2010; Rose et al., 2010; Almeida et
198 al., 2014; Kawana et al., 2016; Cai et al., 2020; Zhang et al., 2020). However, for inorganic/AA and inorganic/OA mixed
199 particles (**Fig. 4b**), their κ_{CCN} values were 0.3-3.0 times higher than κ_{Chem}. Surface tension reduction was one of the potential
200 causes, as discussed in section 3.2 that OA and AA with strong surface activity and low solubilities may result in stronger
201 surface tension reduction than most of the rest dicarboxylic acids. In addition, the underprediction showed a gradual increased
202 trend with increased OVF since increased OVF lead to higher concentration of organics, thus leading to more surface tension
203 reduction. Surface tension reduction in water solution caused by atmospheric surfactants were observed frequently in previous
204 studies (Facchini et al., 1999; Gerard et al., 2016). Results have showed that neglect of surface tension reduction may lead to
205 higher κ_{CCN} values than κ_{Chem} or growth factor derived κ_{GF} (Irwin et al., 2010; Wu et al., 2013; Zhao et al., 2016; Hu et al.,
206 2020; Peng et al., 2021), as well as underpredictions of CCN number concentration (Good et al., 2010; Asa-Awuku et al., 2011;
207 Ovadnevaite et al., 2017; Cai et al., 2020). Hu et al. (2020) reported that κ_{Chem} underpredicted κ_{CCN} by 13% and 18% at
208 supersaturation ratios of 0.1% and 0.3%, which may be attributed to the depression of droplet surface tension by potential
209 surface-active organics. Likewise, Ovadnevaite et al. (2017) only predicted one tenth of measured CCN number concentration
210 in a nascent ultrafine mode event because of the surface tension reduction, and the notable underestimation was improved by
211 applying lower water surface tension (~ 68% of water surface tension) in κ-Köhler theory.
212 Apart from surface tension reduction, aerosol phase states could also bring uncertainty to critical supersaturation and
213 hygroscopicity predictions (Henning et al., 2005; Hodas et al., 2015; Peng et al., 2016; Zhao et al., 2016). Being different from
214 tradition Köhler curve with only one maximum, modified Köhler curve for inorganic salt and slightly soluble dicarboxylic
215 acid (e.g. AA) mixed particles accounting for limited solubility obtained two maxima of critical supersaturation ratios and the
216 higher value among the two maxima determined CCN activation (Bilde and Svenningsson, 2004). The maximum at the larger
217 wet diameter is identical with that obtained by assuming that the organic acids are infinitely soluble in water (i.e. classical

218 Köhler theory). And the other maximum with smaller wet diameter represents the point that all slightly soluble material is

219 fully dissolved and the maximum can also be viewed as an activation barrier which is due to the presence of a undissolved

220 solid part of organic acid (Henning et al., 2005). Pajunoja et al. (2015) reported that biogenic secondary organic aerosol (SOA)

221 particles formed from isoprene showed an increased trend of hygroscopicity parameter from 0.05 to nearly 0.15 when RH

222 increased from 40% to supersaturation. They indirectly found the biogenic SOA to be semisolid phase thus the increased trend

223 of hygroscopicity κ was explained by the gradual phase transition from solid to semisolid (or liquid) with raised RH because

224 water content may gradually wet and dissolve the organic surface and form water film (Pajunoja et al., 2015). The phase

225 transition (or water film formation) of pure OA and AA would be difficult (i.e. high RH is required) because of their high

226 deliquescence point and low solubilities, but could be easier (i.e. required high RH is decreased) by addition of inorganic salts.

227 Overall, phase state and surface tension of atmospheric aerosol were two essential factors influencing their hygroscopicity and

228 CCN activation. Though there are several indirect ways detecting aerosol phase state (Pajunoja et al., 2015; Shiraiwa et al.,

229 2017), current studies about direct measurements are still very limited.

3.4 Phase state and surface tension of inorganic salt/dicarboxylic acid mixed particles

3.4.1 Phase state

232 We obtained phase states of inorganic salt/dicarboxylic acid under high RH (over 99.5%) by analyzing shapes of force plot

233 based on AFM system (Lee et al., 2017a; Lee and Tivanski, 2021). **Figure 5a** shows force plot of NaCl/MA mixed particles

234 with 75% OVF. AFM probe needle tip approached the droplet vertically before contacting with droplet, needle tip was not

235 disturbed by extra force (red line). Then, needle tip came in contact with the droplet, resulting in an abrupt negative force (i.e.

236 needle was attracting by drop). After that, needle moved through the droplet with negative force until contacting with the

237 substrate. When tip contacted substrate, the negative force would quickly be positive (repulsive force), exceeding a predefined

238 maximum amount of force. Then the tip retracted back away from the droplet, as indicates by blue line. Because of the surface

239 tension of droplet surface, needle tip would experience attractive force and abruptly turned to zero when tip separated from

240 droplet surface. Our observation in **Fig. 5a** showed a similar shape with results reported by Morris et al. (2015), indicating the

241 particles were liquid. Most of the studied inorganic salt/dicarboxylic acid (MA, PhMA, SA, PhSA and PA) were liquid under

242 RH over 99.5%.

243 However, for AS/SA (72% and 88% OVF), NaCl/AA (89% OVF), AS/AA (57%, 72% and 88% OVF) and AS/OA (88%

244 OVF), the shape force plots were totally different. During the tip contacting with particle, force plots showing a jagging profile,

245 as shown in **Fig. 5b.** This shape is nearly the same as the curves for NaBr particles under 52% RH reported by Lee et al.

246 (2017a). They explained the phase of NaBr was semi-solid and jagging profile in tip approaching was caused by its viscosity.

247 Therefore, AS/SA (72% and 88% OVF), NaCl/AA (89% OVF), AS/AA (57%, 72% and 88% OVF) and AS/OA (88% OVF)

248 mixed particles were indicated to be semisolid. Semisolid phase states were more likely to occur when containing higher OVF

249 of dicarboxylic acids with lower solubilities and higher deliquescence point (SA, AA and OA) and inorganic salts with

250 comparative lower hygroscopicity (AS), as in this circumstance water content may be insufficient and could not easily dissolve
251 organics. Therefore, semisolid phase of inorganic salt/AA and inorganic salt/OA mixed particles provides evident for phase
252 state effect on aerosol hygroscopicity, which may be attributable to higher κ_{CCN} than κ_{Chem} as discussed in section 3.3 (**Fig 4b**).
253 Though AS/SA mixed particles (72% and 88% OVF) were semisolid because of high deliquescence point (98%) of SA, their
254 good closure between κ_{CCN} and κ_{Chem} may be ascribed to higher solubility of SA, which may intensify the water absorption
255 after deliquescence thus phase transition from semisolid to diluted liquid when activating to CCN.

3.4.2 Surface tension

257 Lee et al. (2017a) pointed out that surface tension calculation could not be achieved for semisolid particles, because the
258 measured retention force was not solely attributed to surface tension, but have additional contributions that include viscosity.
259 Therefore, only surface tensions of inorganic salt/dicarboxylic acid mixed particles that were liquid were further obtained by
260 **Eq.3**. Surface tension results were summarized in **Fig. 6**. Overall, surface tensions of all inorganic salt/dicarboxylic acid mixed
261 particles showed a decrease trend with increased OVF as higher OVF may result in higher organic solute concentrations thus
262 caused more surface tension reduction. Surface tensions of inorganic salts mixed with MA, PhMA, SA, PhSA and PA lowered
263 by within 12% than that of pure water (72 mN m^{-1}), indicating that droplets got strongly diluted at RH over 99.5%, and ought
264 to be more diluted when activation occurs. This may contribute to κ closure within 30% deviation in **Fig. 4a** because diluted
265 solution and water surface tension were assumed in κ-Köhler theory. However, surface tensions of inorganic salts/AA and
266 inorganic salts/OA mixed particles showed notable reductions (20%-42%), which may contribute to their higher κ_{CCN} values
267 than κ_{Chem} (**Fig. 4b**). Besides, notable surface tension reductions of particles containing OA or AA indicated that organic
268 solubility plays an important role in surface tension reduction as AA and OA have the lowest solubilities among studied
269 dicarboxylic acids. OA and AA own higher carbon numbers than most of the rest studied organics. Since Aumann et al. (2010)
270 found that the surface activity of dicarboxylic acids increases with carbon number from 2 to 9 based on surface tension
271 measurement of their water solutions, indicating that dicarboxylic acids (e.g. OA and AA) with higher carbon number own
272 stronger surface activity. Therefore, strong surface activity of dicarboxylic acid is another factor attributing to surface tension
273 reduction of inorganic salts/dicarboxylic acids. In order to quantitively connect in surface tension and measured κ_{CCN}, we used
274 the solubility-involved Köhler model which was introduced by Petters and Kreidenweis (2008), to investigate sensitivity of
275 the measured κ_{CCN} values on the assumed value of surface tension for inorganic salts/OA systems. As shown in **Fig. 7a**, κ_{CCN}
276 of NaCl/OA with 60%, 75% and 89% OVF derived from solubility-involved Köhler model with water surface tension were
277 0.515, 0.324 and 0.145 (circles). These values underpredict measured κ_{CCN} (0.688, 0.485 and 0.296, triangles). However, if
278 modeled κ_{CCN} values fit the measured values, the corresponding surface tensions should reduce to 65.4 mN m^{-1} (60% OVF),
279 62.7 mN m^{-1} (75% OVF), 56.7 mN m^{-1} (89% OVF). Similar results were also found for AS/OA systems (**Fig.7b**). In **Fig. 7c**,
280 fitted surface tension showed good linear relation with measured surface tensions (slope and R^2 were 1.09 and 0.71). Therefore,
281 our results could provide a quantitative way to predict κ_{CCN} values of inorganic salts/OA based on solubility-involved Köhler

model, by using their measured surface tensions results under high RH. This quantitative method should be tested for more chemical systems in the future.

4 Conclusions

The role of surfactants such as dicarboxylic acids in CCN activity were often ignored in aerosol hygroscopicity studies and currently used climate models. In this study, we analyzed CCN activities of inorganic salt/dicarboxylic acid internal mixed particles with varied OVF and directly measured their phase state and surface tension by AFM under relative high RH.

κ_{CCN} values of single dicarboxylic acid were located in the range of 0.003-0.240. A linearly positive correlation between κ_{CCN} and solubility was obtained for slightly dissolved species, while a negative correlation was found between κ_{CCN} and molecular volume for highly soluble species. κ_{CCN} of PhMA and PhSA were lower than those of MA and SA, respectively, revealing that addition of phenyl radical could weaken hygroscopicity of dicarboxylic acid.

For most inorganic salt/dicarboxylic acid (MA, PhMA, SA, PhSA and PA), κ_{CCN} of mixed particles with same OVF showed an overall decrease trend and followed the order of κ_{CCN} values of single dicarboxylic acid. Good closure within 30% relative bias between κ_{CCN} and κ_{Chem} were obtained. On the contrast, our results demonstrate that the semisolid phase state and surface tension reduction (20%-42%) are the potential factors to explain the enhanced CCN activity of inorganic salts/OA and inorganic salts/AA mixed particles. Slightly dissolved dicarboxylic acids with lower solubilities and strong surface activity are more likely to cause notable surface tension depression for inorganic salt/dicarboxylic acid mix particles. Therefore, we proposed that surface tension reduction and phase state should be carefully considered in future models and observations, especially for slightly soluble organics with lower solubilities and strong surface activity.

Data availability. The data used in this paper can be obtained from the corresponding author upon request.

Author contributions. CX did the experiments, analyzed data, plotted the figures and wrote the original draft. BYK contributed data analyzing and discussion, reviewed the manuscript and contributed to fund acquisition. XYC, XLD, XYP and SKY contributed to the instrumentation and discussion. ZNX contributed to the discussion and fund acquisition. HH contributed to the instrumentation, discussion and fund acquisition. ZBW administrated the project, conceptualized the study, reviewed the manuscript and contributed to fund acquisition.

Acknowledgment. The research was supported by National Natural Science Foundation of China (91844301, 42005087, 61974128 and 42005086) and the Fundamental Research Funds for the Central Universities (2018QNA6008). We thank Dr. Lin Liu from Instrumentation and Service Center for Physical Sciences at Westlake University for the supporting in AFM experiments. We likewise thank Changlong Liu, Dr. Ren Zhu and Dr. Zhiwen Liu at Oxford Instruments, Dr. Renwei Mao at Zhejiang university, Dr. Yuzhong Zhang at Westlake University for the discussions about AFM experiment.

Competing interests. The authors declare no competing financial interest.

References

Almeida, G. P., Brito, J., Morales, C. A., Andrade, M. F., and Artaxo, P.: Measured and modelled cloud condensation nuclei (CCN) concentration in Sao Paulo, Brazil: the importance of aerosol size-resolved chemical composition on CCN concentration prediction, Atmos. Chem. Phys., 14, 7559-7572, https://doi.org/10.5194/acp-14-7559-2014, 2014.

Asa-Awuku, A., Moore, R. H., Nenes, A., Bahreini, R., Holloway, J. S., Brock, C. A., Middlebrook, A. M., Ryerson, T. B., Jimenez, J. L., DeCarlo, P. F., Hecobian, A., Weber, R. J., Stickel, R., Tanner, D. J., and Huey, L. G.: Airborne cloud condensation nuclei measurements during the 2006 Texas Air Quality Study, J. Geophys. Res.: Atmos., 116, D11201, https://doi.org/10.1029/2010jd014874, 2011.

Aumann, E., Hildemann, L. M., and Tabazadeh, A.: Measuring and modeling the composition and temperature-dependence of surface tension for organic solutions, Atmos. Environ., 44, 329-337, https://doi.org/10.1016/j.atmosenv.2009.10.033, 2010.

Bhattu, D. and Tripathi, S. N.: CCN closure study: Effects of aerosol chemical composition and mixing state, J Geophys Res-Atmos, 120, 766-783, https://doi.org/10.1002/2014jd021978, 2015.

Bilde, M. and Svenningsson, B.: CCN activation of slightly soluble organics: the importance of small amounts of inorganic salt and particle phase, Tellus B: Chem. Phys. Meteorol., 56, 128-134, https://doi.org/10.3402/tellusb.v56i2.16406, 2004.

Bzdek, B. R., Reid, J. P., Malila, J., and Prisle, N. L.: The surface tension of surfactant-containing, finite volume droplets, Proc. Natl. Acad. Sci. U.S.A., 117, 8335-8343, https://doi.org/10.1073/pnas.1915660117, 2020.

Cai, M., Liang, B., Sun, Q., Zhou, S., Chen, X., Yuan, B., Shao, M., Tan, H., and Zhao, J.: Effects of continental emissions on cloud condensation nuclei (CCN) activity in the northern South China Sea during summertime 2018, Atmos. Chem. Phys., 20, 9153-9167, https://doi.org/10.5194/acp-20-9153-2020, 2020.

Chan, M. N., Kreidenweis, S. M., and Chan, C. K.: Measurements of the hygroscopic and deliquescence properties of organic compounds of different solubilities in water and their relationship with cloud condensation nuclei activities, Environ. Sci. Technol., 42, 3602-3608, https://doi.org/10.1021/es7023252, 2008.

Cheng, Y. F., Su, H., Koop, T., Mikhailov, E., and Poschl, U.: Size dependence of phase transitions in aerosol nanoparticles, Nat. Commun., 6, https://doi.org/10.1038/ncomms6923, 2015.

Dawson, K. W., Petters, M. D., Meskhidze, N., Petters, S. S., and Kreidenweis, S. M.: Hygroscopic growth and cloud droplet activation of xanthan gum as a proxy for marine hydrogels, J. Geophys. Res.: Atmos., 121, 11803–11818, https://doi.org/10.1002/2016jd025143, 2016.

Ding, Q., Wang, J., Chen, X., Liu, H., Li, Q., Wang, Y., and Yang, S.: Quantitative and sensitive SERS platform with analyte enrichment and filtration function, Nano Lett., 20, 7304-7312, https://doi.org/10.1021/acs.nanolett.0c02683, 2020.

Ding, X., Kuang, B., Xiong, C., Mao, R., Xu, Y., Wang, Z., and Hu, H.: A Super High Aspect Ratio Atomic Force Microscopy Probe for Accurate Topography and Surface Tension Measurement, Sens. Actuators, A, 113891, https://doi.org/10.1016/j.sna.2022.113891, 2022.

Dusek, U., Frank, G. P., Hildebrandt, L., Curtius, J., Schneider, J., Walter, S., Chand, D., Drewnick, F., Hings, S., Jung, D., Borrmann, S., and Andreae, M. O.: Size matters more than chemistry for cloud-nucleating ability of aerosol particles, Science, 312, 1375-1378, https://doi.org/10.1126/science.1125261, 2006.

Facchini, M. C., Mircea, M., Fuzzi, S., and Charlson, R. J.: Cloud albedo enhancement by surface-active organic solutes in growing droplets, Nature, 401, 257-259, https://doi.org/10.1038/45758, 1999.

Gerard, V., Noziere, B., Baduel, C., Fine, L., Frossard, A. A., and Cohen, R. C.: Anionic, Cationic, and Nonionic Surfactants in Atmospheric Aerosols from the Baltic Coast at Asko, Sweden: Implications for Cloud Droplet Activation, Environ Sci Technol, 50, 2974-2982, https://doi.org/10.1021/acs.est.5b05809, 2016.

Good, N., Topping, D. O., Allan, J. D., Flynn, M., Fuentes, E., Irwin, M., Williams, P. I., Coe, H., and McFiggans, G.: Consistency between parameterisations of aerosol hygroscopicity and CCN activity during the RHaMBLe discovery cruise, Atmos. Chem. Phys., 10, 3189-3203, https://doi.org/10.5194/acp-10-3189-2010, 2010.

Gunthe, S. S., King, S. M., Rose, D., Chen, Q., Roldin, P., Farmer, D. K., Jimenez, J. L., Artaxo, P., Andreae, M. O., Martin, S. T., and Pöschl, U.: Cloud condensation nuclei in pristine tropical rainforest air of Amazonia: size-resolved measurements and modeling of atmospheric aerosol composition and CCN activity, Atmos. Chem. Phys., 9, 7551-7575, https://doi.org/10.5194/acp-9-7551-2009, 2009.

Han, S., Hong, J., Luo, Q., Xu, H., Tan, H., Wang, Q., Tao, J., Zhou, Y., Peng, L., He, Y., Shi, J., Ma, N., Cheng, Y., and Su, H.: Hygroscopicity of organic compounds as a function of organic functionality, water solubility, molecular weight, and oxidation level, Atmos. Chem. Phys., 22, 3985-4004, https://doi.org/10.5194/acp-22-3985-2022, 2022.

Henning, S., Rosenorn, T., D'Anna, B., Gola, A. A., Svenningsson, B., and Bilde, M.: Cloud droplet activation and surface tension of mixtures of slightly soluble organics and inorganic salt, Atmos. Chem. Phys., 5, 575-582, https://doi.org/10.5194/acp-5-575-2005, 2005.

Hings, S. S., Wrobel, W. C., Cross, E. S., Worsnop, D. R., Davidovits, P., and Onasch, T. B.: CCN activation experiments with adipic acid: effect of particle phase and adipic acid coatings on soluble and insoluble particles, Atmos. Chem. Phys., 8, 3735-3748, https://doi.org/10.5194/acp-8-3735-2008, 2008.

Ho, K. F., Lee, S. C., Ho, S. S. H., Kawamura, K., Tachibana, E., Cheng, Y., and Zhu, T.: Dicarboxylic acids, ketocarboxylic acids, α-dicarbonyls, fatty acids, and benzoic acid in urban aerosols collected during the 2006 Campaign of Air Quality Research in Beijing (CAREBeijing-2006), J. Geophys. Res.: Atmos., 115, D19312, https://doi.org/10.1029/2009jd013304, 2010.

Hodas, N., Zuend, A., Mui, W., Flagan, R. C., and Seinfeld, J. H.: Influence of particle-phase state on the hygroscopic behavior of mixed organic–inorganic aerosols, Atmos. Chem. Phys., 15, 5027-5045, https://doi.org/10.5194/acp-15-5027-2015, 2015.

Hu, D., Liu, D., Zhao, D., Yu, C., Liu, Q., Tian, P., Bi, K., Ding, S., Hu, K., Wang, F., Wu, Y., Wu, Y., Kong, S., Zhou, W., He, H., Huang, M., and Ding, D.: Closure investigation on cloud condensation nuclei ability of processed anthropogenic aerosols, J. Geophys. Res.: Atmos., 125, e2020JD032680, https://doi.org/10.1029/2020jd032680, 2020.

Hyder, M., Genberg, J., Sandahl, M., Swietlicki, E., and Jönsson, J. Å.: Yearly trend of dicarboxylic acids in organic aerosols from south of Sweden and source attribution, Atmos. Environ., 57, 197-204, https://doi.org/10.1016/j.atmosenv.2012.04.027, 2012.

Irwin, M., Good, N., Crosier, J., Choularton, T. W., and McFiggans, G.: Reconciliation of measurements of hygroscopic growth and critical supersaturation of aerosol particles in central Germany, Atmos. Chem. Phys., 10, 11737-11752, https://doi.org/10.5194/acp-10-11737-2010, 2010.

Juranyi, Z., Gysel, M., Weingartner, E., DeCarlo, P. F., Kammermann, L., and Baltensperger, U.: Measured and modelled cloud condensation nuclei number concentration at the high alpine site Jungfraujoch, Atmos. Chem. Phys., 10, 7891-7906, https://doi.org/10.5194/acp-10-7891-2010, 2010.

Kaluarachchi, C. P., Lee, H. D., Lan, Y., Lansakara, T. I., and Tivanski, A. V.: Surface tension measurements of aqueous liquid-air interfaces probed with microscopic indentation, Langmuir, 37, 2457-2465, https://doi.org/10.1021/acs.langmuir.0c03507, 2021.

Kawana, K., Nakayama, T., and Mochida, M.: Hygroscopicity and CCN activity of atmospheric aerosol particles and their relation to organics: Characteristics of urban aerosols in Nagoya, Japan, J. Geophys. Res.: Atmos., 121, 4100-4121, https://doi.org/10.1002/2015jd023213, 2016.

Köhler, H.: The nucleus in and the growth of hygroscopic droplets, Trans. Faraday Soc., 32, 1152-1161, https://doi.org/10.1039/tf9363201152, 1936.

Kumar, P. P., Broekhuizen, K., and Abbatt, J. P. D.: Organic acids as cloud condensation nuclei: Laboratory studies of highly soluble and insoluble species, Atmos. Chem. Phys., 3, 509-520, https://doi.org/10.5194/acp-3-509-2003, 2003.

Kuwata, M., Shao, W., Lebouteiller, R., and Martin, S. T.: Classifying organic materials by oxygen-to-carbon elemental ratio to predict the activation regime of Cloud Condensation Nuclei (CCN), Atmos. Chem. Phys., 13, 5309-5324, https://doi.org/10.5194/acp-13-5309-2013, 2013.

Lee, H. D., Estillore, A. D., Morris, H. S., Ray, K. K., Alejandro, A., Grassian, V. H., and Tivanski, A. V.: Direct surface tension measurements of individual sub-micrometer particles using atomic force microscopy, J. Phys. Chem. A, 121, 8296-8305, https://doi.org/10.1021/acs.jpca.7b04041, 2017a.

Lee, H. D., Ray, K. K., and Tivanski, A. V.: Solid, semisolid, and liquid phase states of individual submicrometer particles directly probed using atomic force microscopy, Anal. Chem., 89, 12720-12726, https://doi.org/10.1021/acs.analchem.7b02755, 2017b.

Lee, H. D., Morris, H. S., Laskina, O., Sultana, C. M., Lee, C., Jayarathne, T., Cox, J. L., Wang, X., Hasenecz, E. S., DeMott, P. J., Bertram, T. H., Cappa, C. D., Stone, E. A., Prather, K. A., Grassian, V. H., and Tivanski, A. V.: Organic enrichment, physical phase state, and surface tension depression of nascent core–shell sea spray aerosols during two phytoplankton blooms, ACS Earth Space Chem., 4, 650-660, https://doi.org/10.1021/acsearthspacechem.0c00032, 2020.

Lee, H. D. and Tivanski, A. V.: Atomic force microscopy: An emerging tool in measuring the phase state and surface tension of individual aerosol particles, Annu. Rev. Phys. Chem., 72, 235-252, https://doi.org/10.1146/annurev-physchem-090419-110133, 2021.

Lee, J. Y. and Hildemann, L. M.: Surface tension of solutions containing dicarboxylic acids with ammonium sulfate, d-glucose, or humic acid, J. Aerosol Sci., 64, 94-102, https://doi.org/10.1016/j.jaerosci.2013.06.004, 2013.

Lee, J. Y. and Hildemann, L. M.: Surface tensions of solutions containing dicarboxylic acid mixtures, Atmos. Environ., 89, 260-267, https://doi.org/10.1016/j.atmosenv.2014.02.049, 2014.

Liu, P. F., Song, M. J., Zhao, T. N., Gunthe, S. S., Ham, S. H., He, Y. P., Qin, Y. M., Gong, Z. H., Amorim, J. C., Bertram, A. K., and Martin, S. T.: Resolving the mechanisms of hygroscopic growth and cloud condensation nuclei activity for organic particulate matter, Nat. Commun., 9, 4076, https://doi.org/10.1038/s41467-018-06622-2, 2018.

Lowe, S. J., Partridge, D. G., Davies, J. F., Wilson, K. R., Topping, D., and Riipinen, I.: Key drivers of cloud response to surface-active organics, Nat. Commun., 10, 5214, https://doi.org/10.1038/s41467-019-12982-0, 2019.

Luo, Q. W., Hong, J., Xu, H. B., Han, S., Tan, H. B., Wang, Q. Q., Tao, J. C., Ma, N., Cheng, Y. F., and Su, H.: Hygroscopicity of amino acids and their effect on the water uptake of ammonium sulfate in the mixed aerosol particles, Sci. Total Environ., 734, 139318, https://doi.org/10.1016/j.scitotenv.2020.139318, 2020.

Metcalf, A. R., Boyer, H. C., and Dutcher, C. S.: Interfacial tensions of aged organic aerosol particle mimics using a biphasic microfluidic platform, Environ. Sci. Technol., 50, 1251-1259, https://doi.org/10.1021/acs.est.5b04880, 2016.

Minambres, L., Mendez, E., Sanchez, M. N., Castano, F., and Basterretxea, F. J.: Water uptake of internally mixed ammonium sulfate and dicarboxylic acid particles probed by infrared spectroscopy, Atmos. Environ., 70, 108-116, https://doi.org/10.1016/j.atmosenv.2013.01.007, 2013.

Moore, R. H. and Nenes, A.: Scanning Flow CCN Analysis—A Method for Fast Measurements of CCN Spectra, Aerosol Sci. Technol., 43, 1192-1207, https://doi.org/10.1080/02786820903289780, 2009.

Morris, H. S., Grassian, V. H., and Tivanski, A. V.: Humidity-dependent surface tension measurements of individual inorganic and organic submicrometre liquid particles, Chem. Sci., 6, 3242-3247, https://doi.org/10.1039/c4sc03716b, 2015.

Nguyen, Q. T., Kjær, K. H., Kling, K. I., Boesen, T., and Bilde, M.: Impact of fatty acid coating on the CCN activity of sea salt particles, Tellus B: Chem. Phys. Meteorol., 69, https://doi.org/10.1080/16000889.2017.1304064, 2017.

Noziere, B.: Don't forget the surface, Science, 351, 1396-1397, https://doi.org/10.1126/science.aaf3253, 2016.

Ovadnevaite, J., Zuend, A., Laaksonen, A., Sanchez, K. J., Roberts, G., Ceburnis, D., Decesari, S., Rinaldi, M., Hodas, N., Facchini, M. C., Seinfeld, J. H., and C, O. D.: Surface tension prevails over solute effect in organic-influenced cloud droplet activation, Nature, 546, 637-641, https://doi.org/10.1038/nature22806, 2017.

Pajunoja, A., Lambe, A. T., Hakala, J., Rastak, N., Cummings, M. J., Brogan, J. F., Hao, L. Q., Paramonov, M., Hong, J., Prisle, N. L., Malila, J., Romakkaniemi, S., Lehtinen, K. E. J., Laaksonen, A., Kulmala, M., Massoli, P., Onasch, T. B., Donahue, N. M., Riipinen, I., Davidovits, P., Worsnop, D. R., Petaja, T., and Virtanen, A.: Adsorptive uptake

453   of water by semisolid secondary organic aerosols, Geophys. Res. Lett., 42, 3063-3068,
454   https://doi.org/10.1002/2015gl063142, 2015.

455 Parsons, M. T., Mak, J., Lipetz, S. R., and Bertram, A. K.: Deliquescence of malonic, succinic, glutaric, and adipic acid
456   particles, J. Geophys. Res.: Atmos., 109, D06212, https://doi.org/10.1029/2003jd004075, 2004.

457 Peng, C., Chan, M. N., and Chan, C. K.: The hygroscopic properties of dicarboxylic and multifunctional acids:
458   Measurements and UNIFAC predictions, Environ. Sci. Technol., 35, 4495-4501, https://doi.org/10.1021/es0107531,
459   2001.

460 Peng, C., Jing, B., Guo, Y. C., Zhang, Y. H., and Ge, M. F.: Hygroscopic behavior of multicomponent aerosols involving
461   NaCl and dicarboxylic Acids, J. Phys. Chem. A, 120, 1029-1038, https://doi.org/10.1021/acs.jpca.5b09373, 2016.

462 Peng, C., Razafindrambinina, P. N., Malek, K. A., Chen, L. X. D., Wang, W. G., Huang, R. J., Zhang, Y. Q., Ding, X.,
463   Ge, M. F., Wang, X. M., Asa-Awuku, A. A., and Tang, M. J.: Interactions of organosulfates with water vapor under
464   sub- and supersaturated conditions, Atmos. Chem. Phys., 21, 7135-7148, https://doi.org/10.5194/acp-21-7135-2021,
465   2021.

466 Peng, C., Chen, L., and Tang, M.: A database for deliquescence and efflorescence relative humidities of compounds with
467   atmospheric relevance, Fundam. Res., 2, 578-587, https://doi.org/10.1016/j.fmre.2021.11.021, 2022.

468 Petters, M. D. and Kreidenweis, S. M.: A single parameter representation of hygroscopic growth and cloud condensation
469   nucleus activity, Atmos. Chem. Phys., 7, 1961-1971, https://doi.org/10.5194/acp-7-1961-2007, 2007.

470 Petters, M. D., and Kreidenweis, S. M.: A single parameter representation of hygroscopic growth and cloud condensation
471   nucleus activity - Part 2: Including solubility, Atmos. Chem. Phys., 8, 6273-6279, 10.5194/acp-8-6273-2008, 2008.

472 Petters, M. D., Kreidenweis, S. M., Prenni, A. J., Sullivan, R. C., Carrico, C. M., Koehler, K. A., and Ziemann, P. J.:
473   Role of molecular size in cloud droplet activation, Geophys. Res. Lett., 36, https://doi.org/10.1029/2009gl040131,
474   2009.

475 Petters, S. S., Pagonis, D., Claflin, M. S., Levin, E. J. T., Petters, M. D., Ziemann, P. J., and Kreidenweis, S. M.:
476   Hygroscopicity of organic compounds as a function of carbon chain length and carboxyl, hydroperoxy, and carbonyl
477   functional groups, J. Phys. Chem. A, 121, 5164-5174, https://doi.org/10.1021/acs.jpca.7b04114, 2017.

478 Ray, K. K., Lee, H. D., Gutierrez, M. A., Jr., Chang, F. J., and Tivanski, A. V.: Correlating 3D morphology, phase state,
479   and viscoelastic properties of individual substrate-deposited particles, Anal. Chem., 91, 7621-7630,
480   https://doi.org/10.1021/acs.analchem.9b00333, 2019.

481 Römpp, A., Winterhalter, R., and Moortgat, G. K.: Oxodicarboxylic acids in atmospheric aerosol particles, Atmos.
482   Environ., 40, 6846-6862, https://doi.org/10.1016/j.atmosenv.2006.05.053, 2006.

483 Rose, D., Gunthe, S. S., Mikhailov, E., Frank, G. P., Dusek, U., Andreae, M. O., and Pöschl, U.: Calibration and
484   measurement uncertainties of a continuous-flow cloud condensation nuclei counter (DMT-CCNC): CCN activation
485   of ammonium sulfate and sodium chloride aerosol particles in theory and experiment, Atmos. Chem. Phys., 8, 1153-
486   1179, https://doi.org/10.5194/acp-8-1153-2008, 2008.

487 Rose, D., Nowak, A., Achtert, P., Wiedensohler, A., Hu, M., Shao, M., Zhang, Y., Andreae, M. O., and Pöschl, U.:
488   Cloud condensation nuclei in polluted air and biomass burning smoke near the mega-city Guangzhou, China – Part
489   1: Size-resolved measurements and implications for the modeling of aerosol particle hygroscopicity and CCN
490   activity, Atmos. Chem. Phys., 10, 3365-3383, https://doi.org/10.5194/acp-10-3365-2010, 2010.

491 Rosenfeld, D., Sherwood, S., Wood, R., and Donner, L.: Climate effects of aerosol-cloud interactions, Science, 343,
492   379-380, https://doi.org/10.1126/science.1247490, 2014.

493 Ruehl, C. R., Chuang, P. Y., and Nenes, A.: Aerosol hygroscopicity at high (99 to 100%) relative humidities, Atmos.
494   Chem. Phys., 10, 1329-1344, https://doi.org/10.5194/acp-10-1329-2010, 2010.

495 Ruehl, C. R., Chuang, P. Y., Nenes, A., Cappa, C. D., Kolesar, K. R., and Goldstein, A. H.: Strong evidence of surface
496   tension reduction in microscopic aqueous droplets, Geophys. Res. Lett., 39, L23801,
497   https://doi.org/10.1029/2012gl053706, 2012.

498 Ruehl, C. R. and Wilson, K. R.: Surface organic monolayers control the hygroscopic growth of submicrometer particles
499   at high relative humidity, J. Phys. Chem. A, 118, 3952-3966, https://doi.org/10.1021/jp502844g, 2014.

Ruehl, C. R., Davies, J. F., and Wilson, K. R.: An interfacial mechanism for cloud droplet formation on organic aerosols, Science, 351, 1447-1450, https://doi.org/10.1126/science.aad4889, 2016.

Shiraiwa, M., Li, Y., Tsimpidi, A. P., Karydis, V. A., Berkemeier, T., Pandis, S. N., Lelieveld, J., Koop, T., and Poschl, U.: Global distribution of particle phase state in atmospheric secondary organic aerosols, Nat. Commun., 8, 15002, https://doi.org/10.1038/ncomms15002, 2017.

Sjogren, S., Gysel, M., Weingartner, E., Baltensperger, U., Cubison, M. J., Coe, H., Zardini, A. A., Marcolli, C., Krieger, U. K., and Peter, T.: Hygroscopic growth and water uptake kinetics of two-phase aerosol particles consisting of ammonium sulfate, adipic and humic acid mixtures, J. Aerosol Sci., 38, 157-171, https://doi.org/10.1016/j.jaerosci.2006.11.005, 2007.

Suda, S. R., Petters, M. D., Yeh, G. K., Strollo, C., Matsunaga, A., Faulhaber, A., Ziemann, P. J., Prenni, A. J., Carrico, C. M., Sullivan, R. C., and Kreidenweis, S. M.: Influence of functional groups on organic aerosol cloud condensation nucleus activity, Environ. Sci. Technol., 48, 10182-10190, https://doi.org/10.1021/es502147y, 2014.

Vepsäläinen, S., Calderón, S. M., Malila, J., and Prisle, N. L.: Comparison of six approaches to predicting droplet activation of surface active aerosol – Part 1: moderately surface active organics, Atmos. Chem. Phys., 22, 2669-2687, https://doi.org/10.5194/acp-22-2669-2022, 2022.

Wu, Z. J., Poulain, L., Henning, S., Dieckmann, K., Birmili, W., Merkel, M., van Pinxteren, D., Spindler, G., Müller, K., Stratmann, F., Herrmann, H., and Wiedensohler, A.: Relating particle hygroscopicity and CCN activity to chemical composition during the HCCT-2010 field campaign, Atmos. Chem. Phys., 13, 7983-7996, https://doi.org/10.5194/acp-13-7983-2013, 2013.

Yazdanpanah, M. M., Hosseini, M., Pabba, S., Berry, S. M., Dobrokhotov, V. V., Safir, A., Keynton, R. S., and Cohn, R. W.: Micro-wilhelmy and related liquid property measurements using constant-diameter nanoneedle-tipped atomic force microscope probes, Langmuir, 24, 13753-13764, https://doi.org/10.1021/la802820u, 2008.

Zhang, C., Bu, L., Fan, F., Ma, N., Wang, Y., Yang, Y., Größ, J., Yan, J., and Wiedensohler, A.: Surfactant effect on the hygroscopicity of aerosol particles at relative humidity ranging from 80% to 99.5%: Internally mixed adipic acid-ammonium sulfate particles, Atmos. Environ., 266, 118725−118736, https://doi.org/10.1016/j.atmosenv.2021.118725, 2021.

Zhang, Y., Tao, J., Ma, N., Kuang, Y., Wang, Z., Cheng, P., Xu, W., Yang, W., Zhang, S., Xiong, C., Dong, W., Xie, L., Sun, Y., Fu, P., Zhou, G., Cheng, Y., and Su, H.: Predicting cloud condensation nuclei number concentration based on conventional measurements of aerosol properties in the North China Plain, Sci. Total Environ., 719, 137473, https://doi.org/10.1016/j.scitotenv.2020.137473, 2020.

Zhao, D. F., Buchholz, A., Kortner, B., Schlag, P., Rubach, F., Fuchs, H., Kiendler-Scharr, A., Tillmann, R., Wahner, A., Watne, Å. K., Hallquist, M., Flores, J. M., Rudich, Y., Kristensen, K., Hansen, A. M. K., Glasius, M., Kourtchev, I., Kalberer, M., and Mentel, T. F.: Cloud condensation nuclei activity, droplet growth kinetics, and hygroscopicity of biogenic and anthropogenic secondary organic aerosol (SOA), Atmos. Chem. Phys., 16, 1105-1121, https://doi.org/10.5194/acp-16-1105-2016, 2016.

537 **Table 1. Substances and their relevant properties investigated in this study.**

Compounds	Molar weight (g mol^{-1})	Density (g cm^{-3})	Solubility (g L^{-1})	DRH (%RH)	Purity	Supplier
NaCl	58.44[a]	2.16[a]	360[b]	73-77[c]	≥99.8 %	Sinopharm Chemical Reagent
AS	132.13[a]	1.77[a]	770[b]	78-82[c]	≥99%	Sigma Aldrich
MA	104.06[a]	1.63[a]	1400[b]	65-76[c]	≥99%	Sigma Aldrich
PhMA	180.16[a]	1.40[a]	131[a]	NA	98%	Aladdin
SA	118.09[a]	1.57[a]	80[b]	98[d]	≥99%	Aladdin
PhSA	194.19[a]	1.13[a]	241[a]	NA	98%	Macklin
AA	146.14[a]	1.36[a]	14.4[b]	~100[e]	≥99.8 %	Sinopharm Chemical Reagent
PA	160.17[a]	1.28[a]	25[b]	>90[c]	99%	Macklin
OA	174.20[a]	1.16[a]	12[a]	>90[c]	99%	Aladdin

538 [a] https://comptox.epa.gov/ (last access: 3rd August 2022). [b] https://www.chemicalbook.com/ (last access: 3rd August 2022). [c]
539 Peng et al. (2022) and references therein. [d] Peng et al. (2001). [e] Parsons et al. (2004). DRH means deliquescence RH. NA
540 indicates no reported results are available.

541

542 **Table 2. Summary of κ_{CCN} for single component particles.**

Chemicals	D_d (nm)	κ_{CCN} mean ± standard deviation	Previous reported κ_{CCN}
NaCl	50, 65, 76, 88, 100	1.325 ± 0.038	1.28[a]
AS	50, 65, 76, 88, 100	0.562 ± 0.059	0.61[a]
MA	50, 65, 76, 88, 100	0.240 ± 0.036	0.227[a]
PhMA	50, 65, 76, 88, 100	0.183 ± 0.032	NA
SA	50, 65, 76, 88, 100	0.204 ± 0.023	0.166-0.295[a]
PhSA	50, 65, 76, 88, 100	0.145 ± 0.017	NA
AA	140, 160, 180, 200	0.008 ± 0.001	0.005-0.008[b]
PA	65, 76, 88, 100	0.112 ± 0.010	0.14[b]
OA	200, 220, 240, 260	0.003 ± 0.0002	0.001[b]

543 [a] Petters et al., 2007; [b] Kuwata et al. (2013) and references therein. NA indicates no reported results are available.

544

545

546
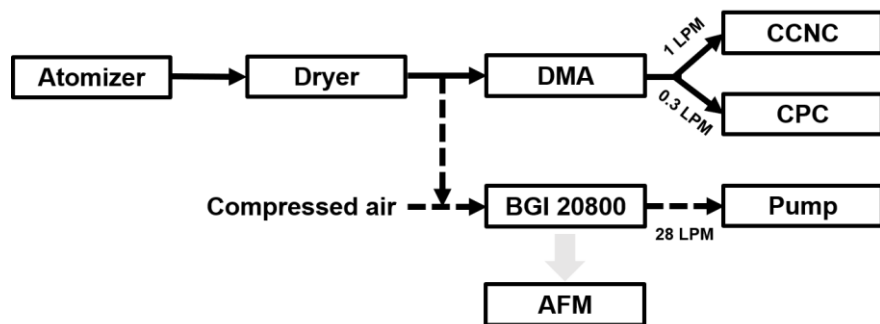
Figure 1: Schematic illustration of the instrumental set-up. The arrow indicates the flow direction. LPM means liter per minute.

548

549
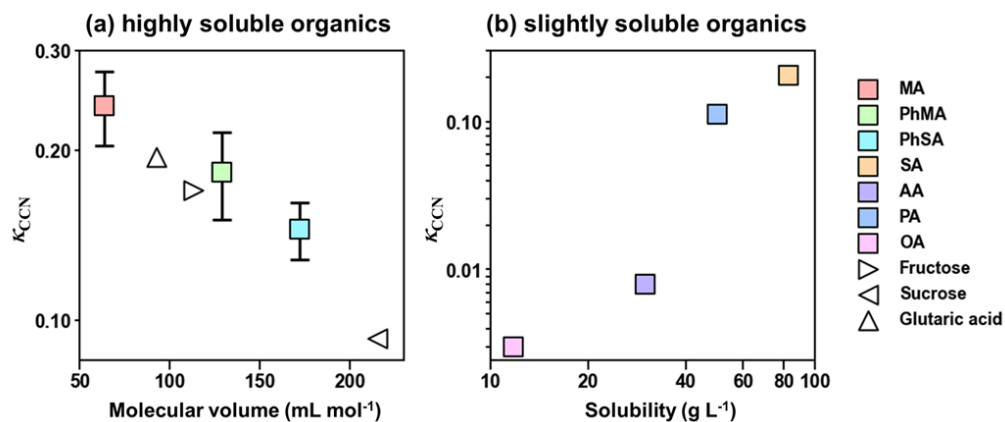
Figure 2: κ_{CCN} of organic compounds as a function of (a) molecular volume and (b) solubility. Solid squares represent κ_{CCN} results in this study while hollow triangles were κ_{CCN} results obtained from Chan et al. (2008).

552

553
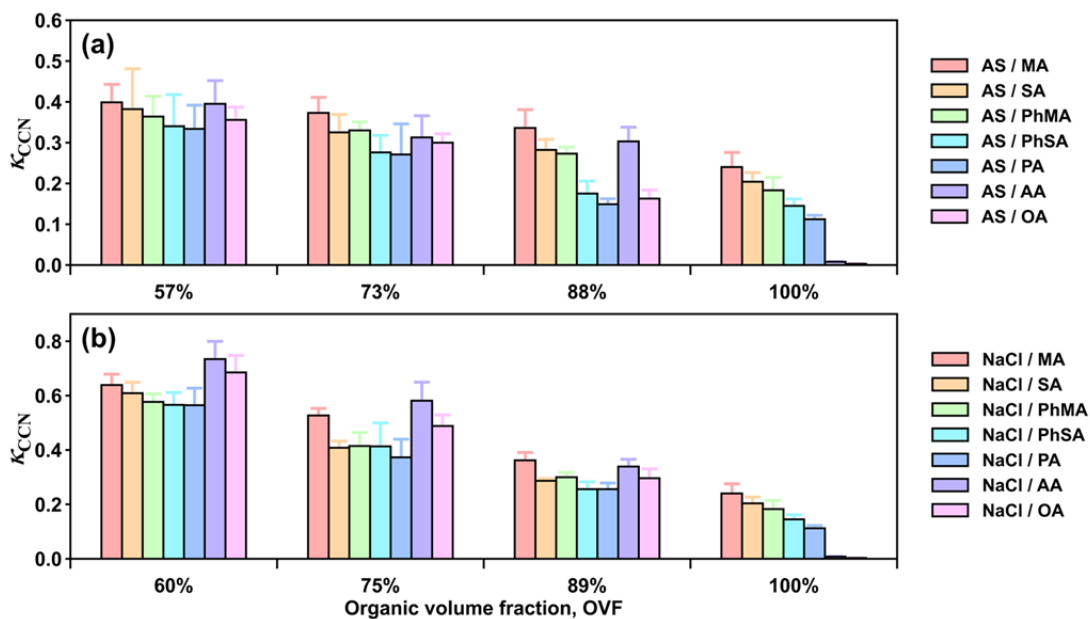
554   **Figure 3:** κ_{CCN} **of (a) AS/dicarboxylic acid and (b) NaCl/dicarboxylic acid mixed particles with varied OVF.**

555
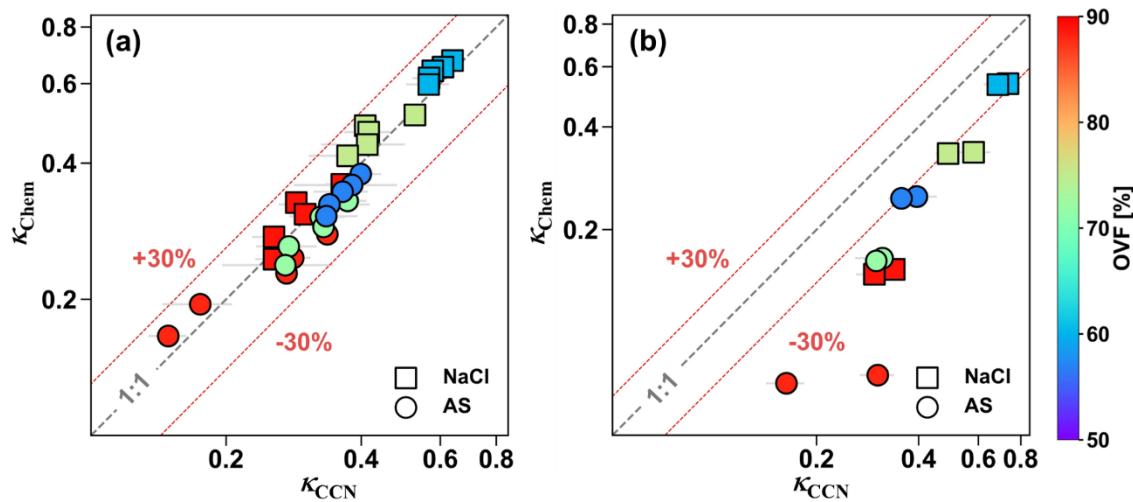
556

557   **Figure 4: Comparison between κ_{CCN} and κ_{Chem} of (a) inorganic salt mixed with MA, PhMA, SA, PhSA and PA (b) inorganic salt**
558   **mixed with AA and OA. Square represents NaCl containing particles and circle represents AS containing particles. Color bar**
559   **indicates OVF.**

560

561
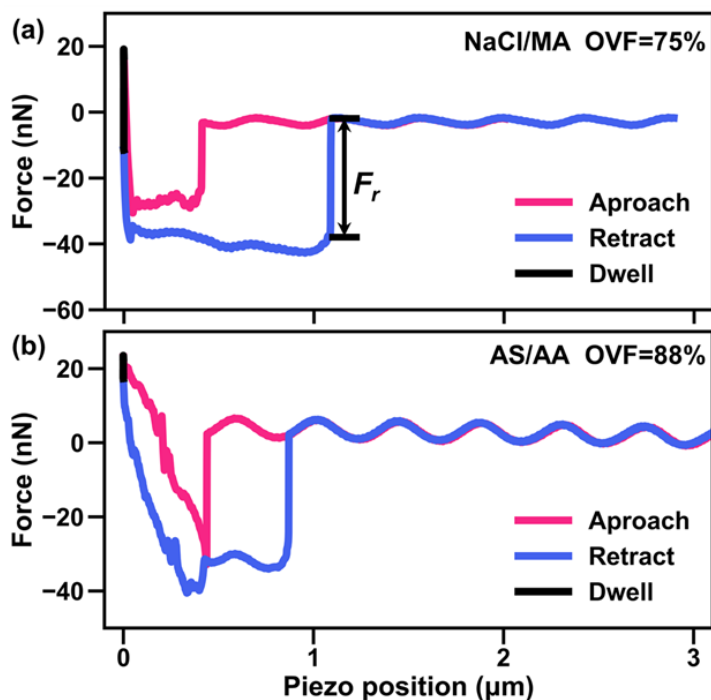
Figure 5: AFM force plots of (a) NaCl/MA system with 75% OVF and (b) AS/AA system with 88% OVF. F_r is the retention force to break the meniscus by the tip of AFM probe.

564
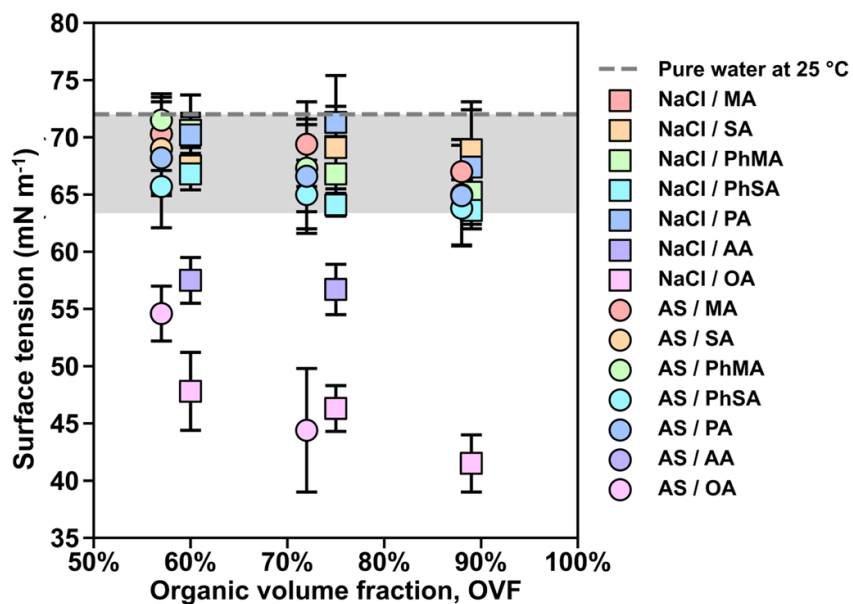
Figure 6: Measured surface tension values of inorganic salt/dicarboxylic acid particles under RH over 99.5%. Gray area covers the surface tension reductions below 12% comparing with pure water (72 mN m^{-1}).

567
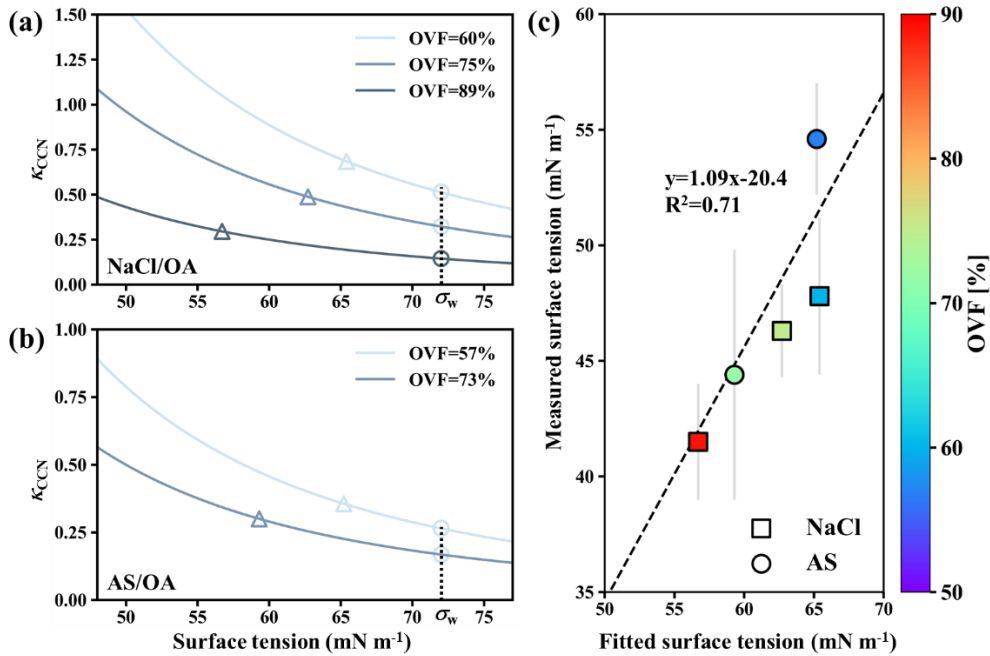
Figure 7: κ_{CCN} vs. assumed surface tension for (a) NaCl/OA and (b) AS/OA systems according to solubility-involved Köhler model presented by Petters and Kreidenweis (2008). The triangles and circles in (a) and (b) represent the measured κ_{CCN} and predict κ_{CCN} by solubility-involved Köhler model. Closure between fitted surface tensions and measured surface tensions (c). σ_w represents water surface tension (72 mN m^{-1}).

572

573

574